

# Graphical Abstract

## Decoding Neural Emotion Patterns through Large Language Model Embeddings

Gideon Vos, Maryam Ebrahimpour, Liza van Eijk, Zoltan Sarnyai, Mostafa Rahimi Azghadi

5

### Decoding Neural Emotion Patterns through Large Language Model Embeddings

1



This study introduces a computational framework for directly mapping natural language emotional content to brain regions without requiring neuroimaging.

2



The framework demonstrated high spatial specificity by accurately mapping discrete emotions to neuro-anatomically plausible brain regions.

3



Regional assignment patterns from textual data showed strong consistency with established neuroimaging research.

4



The integration of semantic embeddings and neuro-anatomical mapping successfully differentiated between healthy and depressed populations through distinct activation patterns.

## Highlights

### **Decoding Neural Emotion Patterns through Large Language Model Embeddings**

Gideon Vos, Maryam Ebrahimpour, Liza van Eijk, Zoltan Sarnyai, Mostafa Rahimi Azghadi

- This study introduces a computational framework for directly mapping natural language emotional content to brain regions without requiring neuroimaging.
- The integration of semantic embeddings and neuro-anatomical mapping successfully differentiated between healthy and depressed populations through distinct activation patterns.
- The framework demonstrated high spatial specificity by accurately mapping discrete emotions to neuro-anatomically plausible brain regions.
- Regional assignment patterns showed strong consistency with established neuroimaging research.
- In favor of reproducible research and to advance the field, all programming code/data used in this study is made publicly available.

# Decoding Neural Emotion Patterns through Large Language Model Embeddings

Gideon Vos<sup>a</sup>, Maryam Ebrahimpour<sup>a</sup>, Liza van Eijk<sup>b</sup>, Zoltan Sarnyai<sup>c</sup>,  
Mostafa Rahimi Azghadi<sup>a</sup>

<sup>a</sup>*College of Science and Engineering, James Cook University, James Cook  
Dr, Townsville, 4811, QLD, Australia*

<sup>b</sup>*College of Health Care Sciences, James Cook University, James Cook  
Dr, Townsville, 4811, QLD, Australia*

<sup>c</sup>*College of Public Health, Medical, and Vet Sciences, James Cook University, James  
Cook Dr, Townsville, 4811, QLD, Australia*

---

## Abstract

Linking emotional expression in natural language to brain function remains a central challenge in neuroscience and affective computing. While neuroimaging offers insight into emotion localization, it is costly and limited to controlled settings. In this study, we introduce a computational framework that maps textual emotional content to neuroanatomical brain regions, enabling scalable, imaging-free emotionbrain research. Our proposed method combines semantic embeddings, dimensionality reduction, and clustering to identify emotional states, which are mapped onto brain regions associated with affective processing. We applied this framework across three experiments: i) comparing conversational data from healthy and depressed individuals, ii) analyzing a large-scale emotion dataset, and iii) contrasting human language with outputs from a large language model. Emotional intensity was quantified using a lexical scoring system sensitive to keywords, syntax, and modifiers. This approach produced neuro-anatomically plausible mappings with high spatial specificity. Depressed subjects exhibited reduced engagement of the left insula and raphe nuclei, regions linked to interoceptive awareness and serotonergic function. The framework reliably differentiated discrete emotions and revealed that LLM-generated texts, while capturing basic affective patterns, lacked the nuanced activation seen in human language, particularly in empathy and self-referential regions such as the medial prefrontal and posterior cingulate cortices. This work establishes a scalable, cost-effective alternative to neuroimaging, advancing both clinical and com-

putational models of emotion, while providing a neuro-inspired benchmark for assessing how closely AI-generated language mirrors human emotional expression.

*Keywords:* Artificial Intelligence, Mental Health, Depression

*PACS:* 07.05.Mh, 87.19.La

*2000 MSC:* 68T01, 92-08

---

## 1. Introduction

Understanding the neural correlates of emotion has traditionally relied on neuroimaging modalities such as electroencephalography (EEG) and functional magnetic resonance imaging (fMRI) [1–3]. These techniques have revealed the involvement of regions like the amygdala, insula, anterior cingulate cortex, and prefrontal cortex across different emotional states [4]. Meta-analyses of neuroimaging studies have consistently identified these key regions across diverse emotional paradigms, with the amygdala showing particular importance for threat detection and fear processing [5], while the anterior cingulate cortex and insula demonstrate critical roles in emotional awareness and interoceptive processing [6, 7]. However, traditional neuroimaging approaches face significant limitations, including high costs, restricted accessibility, controlled laboratory requirements, and limited ecological validity when studying naturalistic emotional expression [8, 9]. The increasing availability of digital text data presents unprecedented opportunities for emotion-brain mapping that could overcome these existing constraints.

Caucheteux *et al.* [10] demonstrated that large language model (LLM) embeddings align with human brain activity without fine-tuning, showing that pre-trained language models inherently capture aspects of neural language representations. This foundational work was extended by Toneva *et al.* [11], who introduced the concept of brain embeddings, highlighting the geometric alignment between the representational spaces of LLMs and brain activity during reading and listening tasks.

Further evidence of this alignment comes from Schrimpf *et al.* [12], who showed that artificial neural networks, especially transformer-based architectures as used in LLMs, can predict human neural responses to language with remarkable accuracy. These findings collectively support the feasibility of

leveraging LLM-derived embeddings to model brain activity, suggesting that the semantic representations learned by these models may reflect fundamental aspects of how the human brain processes language and emotion.

Parallel efforts have explored mapping emotional text representations to neuro-biological substrates. Tomasino *et al.* [13] developed a cognitive-affective framework demonstrating how emotionally charged linguistic input recruits distinct neural systems, while Chen *et al.* [14] correlated sentiment analysis outputs with fMRI patterns, confirming the brain’s differentiation of emotional valence during narrative comprehension. These studies build upon earlier work demonstrating that emotional processing involves distributed neural networks, with positive emotions preferentially engaging left prefrontal regions and negative emotions showing stronger right hemisphere activation [15].

Zhou *et al.* [16] extended this work by associating semantic embeddings from emotional narratives with fMRI-derived brain states, particularly noting strong alignment in medial prefrontal and temporal regions. Similarly, Xiao *et al.* [17] applied unsupervised clustering on emotion-labeled text to uncover latent emotional dimensions and correlated them with EEG and fMRI features. These computational approaches align with neuroimaging meta-analyses showing that different emotional categories activate distinct but overlapping brain networks, with cognitive emotions recruiting prefrontal cortical areas [18, 19].

The utility of natural text has been further emphasized by Hoemann *et al.* [20], who highlighted the value of social media and dialogue data for studying emotion in real-world contexts. Their findings support using large-scale spontaneous language datasets to infer affective brain states, moving beyond the artificial constraints of laboratory-based emotion elicitation paradigms. This approach is particularly relevant given further research showing that naturalistic emotional expression differs significantly from laboratory-induced emotions in both linguistic patterns and associated neural activity [20].

Despite these advances, existing studies have not established a fully computational, imaging-free method that directly links textual emotional content to specific neuro-anatomical regions. Current approaches typically require either controlled laboratory settings that limit validity, or a focus on general

emotional dimensions rather than specific brain region mapping [8].

This represents a significant gap in our ability to study emotional processing at scale. The motivation for developing a purely computational emotion-brain mapping framework, therefore, stems from several converging factors. First, the exponential growth of digital text data offers an unprecedented window into human emotional expression in naturalistic contexts [20]. Second, advances in semantic embedding technologies have created powerful tools for capturing nuanced relationships between language, meaning, and affective content. Third, decades of neuroimaging research have established a robust understanding of the neuro-anatomical basis of emotion processing, with meta-analytic evidence highlighting key neural circuits involved in emotional regulation and expression [18, 21].

The theoretical foundation of our proposed approach rests on the principle that emotional expression in language reflects underlying neural processes. This hypothesis is supported by evidence showing that the human brain encodes language through distributed, continuous representations [22–24]. Studies have demonstrated a direct alignment between high-dimensional language model embeddings and neural activation patterns in language-processing regions [23–25].

Recent work by Goldstein *et al.* [26] further established that simple linear encoding models can reliably map language model embeddings onto brain activity during natural conversation, achieving robust correlations with recorded signals. Their findings showed that deep embeddings consistently outperform traditional symbolic linguistic features (e.g., phonemes, syntactic categories) in predicting neural responses across cortical regions, suggesting that high-dimensional continuous representations more faithfully reflect the brain’s internal language mechanisms. Importantly, they also revealed individual and regional differences in neural embedding alignment, underscoring the capacity of computational models to capture variability in neural organization that extends beyond region-specific specialization. Such evidence not only validates embedding-based approaches for brain-language mapping but also provides a methodological and theoretical foundation for extending this framework to emotion, where capturing both shared and individual patterns of neural processing is particularly critical.

Furthermore, individuals with certain mental health conditions may exhibit distinct language patterns, including variations in word choice, emotional tone, and syntactic complexity that correlate with well-documented neurobiological abnormalities [8, 27–32]. Extending this perspective, characteristic language patterns in clinical populations may manifest as distinct clusters within embedding space, reflecting altered cognitive and affective processing [31, 33–35]. If these deviations also correspond to measurable shifts in brain activation, embedding-based models could offer novel insights into brain-language relationships and help inform computational mental health diagnostics.

Beyond clinical contexts, this framework could further support advanced applications in areas such as LLM-generated text detection [36], where subtle differences in linguistic patterns, coherence, and semantic clustering could indicate non-human authorship.

This study, therefore, investigates whether it is possible to computationally map natural language emotional expressions directly to brain regions without neuroimaging data, using semantic embeddings and clustering techniques to bridge text analysis with neuro-anatomical mapping. Specifically, we aim to:

- Develop a novel computational framework that transforms textual emotional content into neuro-anatomically plausible brain region activations using state-of-the-art natural language processing embedding techniques.
- Validate the clinical utility of this approach by demonstrating its ability to differentiate between healthy and depressed populations through distinct emotional brain mapping patterns, building on established neuroimaging differences in depression.
- Demonstrate discrete emotion localization by mapping specific emotional states to neuro-anatomically appropriate brain regions with high spatial specificity, consistent with established emotion-brain mapping literature.
- Provide an objective, brain-based measure of human-likeness in language by comparing LLM-generated and human-authored texts through their inferred emotional brain activation patterns.

By providing a cost-effective, scalable alternative to traditional neuroimaging methods, such a computational approach can open new avenues for understanding the neural basis of human emotional communication in digital environments, while maintaining the ability to generate interpretable, neuro-anatomically grounded predictions from textual data alone.

## 2. Methods

### 2.1. Datasets

Three text-based datasets were employed in this study (Table 1). The DIAC-WOZ dataset [37] comprises annotated interview transcripts from individuals diagnosed with depression and healthy controls. The GoEmotions dataset [38] includes 58,000 Reddit [39] comments manually labeled into 27 emotion categories (or neutral). The Schema-Guided Dialogue dataset [40] represents nearly half a million sentences comprised of human and LLM chatbot interactions. All datasets consist of texts produced by native English speakers.

Table 1: Datasets utilized in this study.

Dataset	Emotions	Subjects
DAICWOZ[37]	Healthy and Depressed Categories	134 Clinical interview transcripts
GoEmotions [38]	27 Emotion Categories	58k English Reddit comments
The Schema-Guided Dialogue Dataset [40]	Human and Chat bot conversations	463,282 English sentences

### 2.2. Text Preprocessing and Embedding Generation

During preprocessing (Figure 1, step 1), text was segmented into chunks of approximately 300 characters using periods as sentence boundaries. Next, text embeddings were generated using OpenAIs [41] *text-embedding-ada-002* model (Figure 1, step 2), which produces 1536-dimensional vector representations of input text. This model was chosen for its strong performance in capturing both semantic relationships and emotional nuances in natural language [29–32]. Although training a custom embeddings model for our experimentation is technically feasible, it could introduce unwanted bias into our experiments, while the OpenAI *text-embedding-ada-002* embeddings are commonly used in many public and commercial LLMs. The programming pseudo-code for steps 1 and 2 of Fig. 1 is shown in Algorithm 1.

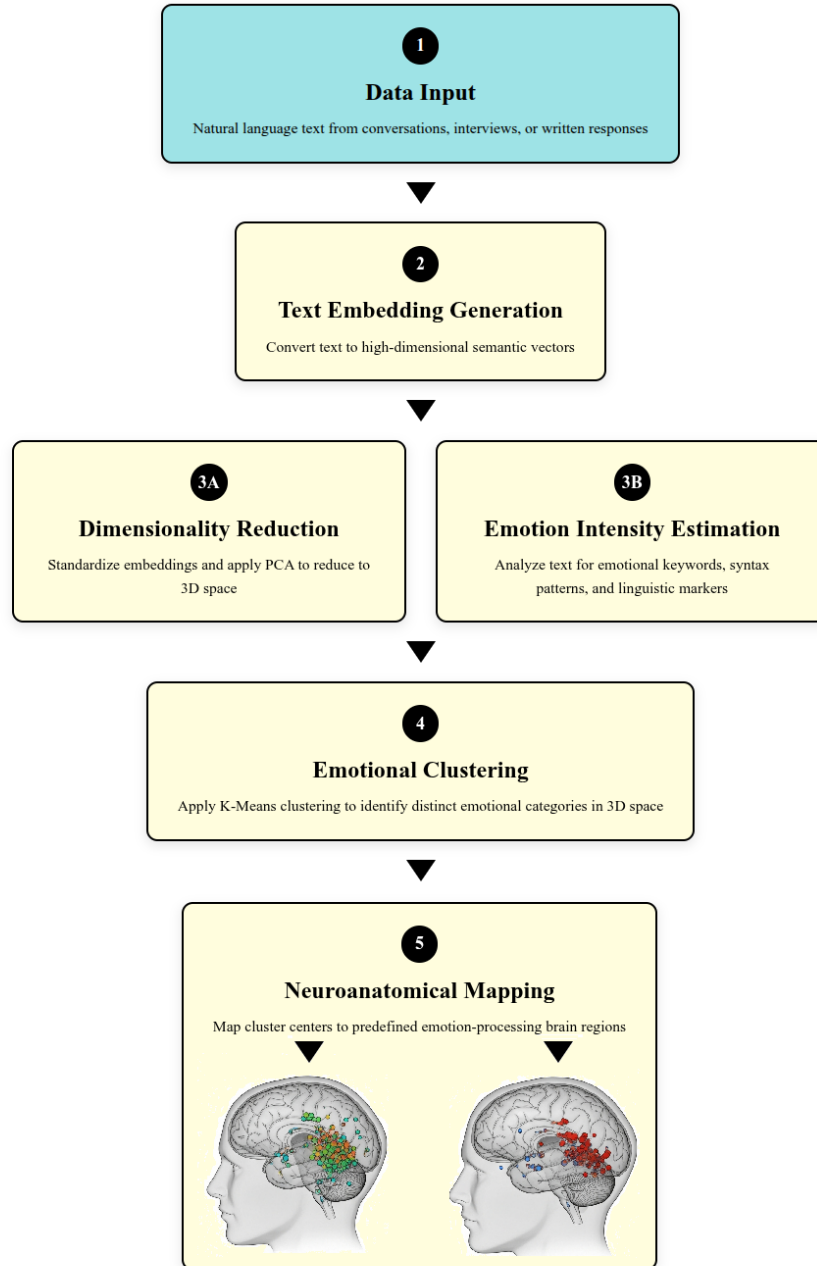


Figure 1: Five-step computational pipeline to convert natural language text to embeddings, reduce dimensionality, cluster to emotional groups and map to brain regions.

---

**Algorithm 1** Text Preprocessing and Embedding Generation

---

**Input:** Text datasets  $D = \{d_1, d_2, d_3\}$

**Output:** 1536-dimensional embeddings matrix

```
1: // Step 1: Text Preprocessing and Chunking
2: function PREPROCESSTEXTS(texts)
3:   chunks  $\leftarrow$  []
4:   for each text in texts do
5:     segments  $\leftarrow$  split text into  $\approx$ 300 character chunks using periods
6:     chunks.append(segments)
7:   end for
8:   return chunks
9: end function
10:
11: // Step 2: Text Embedding Generation
12: function GETADAEMBEDDINGS(texts)
13:   Initialize OpenAI client with API key
14:   embeddings  $\leftarrow$  [], batch_size  $\leftarrow$  2000
15:   for  $i = 0$  to  $\text{len}(\textit{texts})$  step batch_size do
16:     batch  $\leftarrow$  texts[ $i : i + \textit{batch\_size}$ ]
17:     response  $\leftarrow$  client.embeddings.create(model="text-embedding-ada-002", input=batch)
18:     batch_embeddings  $\leftarrow$  extract embeddings from response
19:     embeddings.extend(batch_embeddings)
20:   end for
21:   return  $\textit{np.array}(\textit{embeddings})$  // Shape: (n_samples, 1536)
22: end function
```

---

### 2.3. Dimensionality Reduction and Spatial Mapping

The high-dimensional embeddings underwent a dimensionality reduction process (Figure 1, step 3A) using Principal Component Analysis (PCA) to reduce the dimensionality to three components, representing the minimum number of dimensions required for spatial brain mapping.

### 2.4. Emotional Intensity Estimation

Emotional intensity was quantified using a lexicon-based approach [42–47] combined with syntactic feature analysis (Figure 1, step 3B). This emotion lexicon was constructed containing multiple terms across intensity levels:

- Extreme intensity (1.0): Terms indicating maximum emotional activation (e.g., "devastated," "euphoric," "depressed," "extremely")
- High intensity (0.8): Strong emotional indicators (e.g., "amazing," "hate," "terrible")
- Moderate intensity (0.6): Common emotional expressions (e.g., "love," "sad," "happy")
- Mild intensity (0.3): Subtle emotional content (e.g., "nice," "bad," "okay")

Additional intensity modifiers were incorporated to capture amplification effects:

- Intensification modifiers ("so," "very," "really," "truly," "completely," "totally") added 0.3 to base intensity
- Absolutist terms ("never," "always," "everything," "nothing") contributed 0.2 additional intensity
- Exclamation marks added 0.25 per occurrence (maximum 4)
- Question marks contributed 0.15 per occurrence (maximum 3)
- All-caps text (more than 3 characters) added 0.5 intensity

Base intensity was set at 0.1 for all texts to account for implicit emotional content, with final intensity scores capped at 2.0 to prevent extreme outliers from skewing subsequent analyses. The programming pseudo-code for steps 3A and 3B of Fig. 1 is shown in Algorithm 2.

---

**Algorithm 2** Dimensionality Reduction and Emotional Intensity Estimation

---

**Input:** High-dimensional embeddings from Step 2.

**Output:** 3D embeddings and intensity scores

```
1: // Step 3A: Dimensionality Reduction
2: function FITTRANSFORMEMBEDDINGS(embeddings)
3:   n_components  $\leftarrow$  min(3, n_samples, n_features)
4:   Initialize StandardScaler() and PCA(n_components)
5:   embeddings_scaled  $\leftarrow$  scaler.fit_transform(embeddings)
6:   embeddings_3d  $\leftarrow$  pca.fit_transform(embeddings_scaled)
7:   if embeddings_3d.shape[1] < 3 then
8:     Pad with zeros to ensure 3D representation
9:   end if
10:  return embeddings_3d
11: end function
12:
13: // Step 3B: Emotional Intensity Estimation
14: function ESTIMATEEMOTIONINTENSITY(texts)
15:  Define word_scores: Extreme (1.0), High (0.8), Moderate (0.6), Mild
    (0.3)
16:  intensities  $\leftarrow$  []
17:  for each text in texts do
18:    intensity  $\leftarrow$  0.1, words  $\leftarrow$  extract words from text.lower()
19:    for each word in words do
20:      intensity  $\leftarrow$  intensity + word_scores.get(word, 0)
21:    end for
22:    Apply modifiers: +0.3 (intensifiers), +0.2 (absolutists)
23:    intensity  $\leftarrow$  intensity + 0.25  $\times$  min(text.count('!'), 4)
24:    intensity  $\leftarrow$  intensity + 0.15  $\times$  min(text.count('?'), 3)
25:    if text.isupper() and len(text) > 3 then intensity  $\leftarrow$  intensity +
    0.5
26:    end if
27:    intensities.append(min(intensity, 2.0))
28:  end for
29:  return np.array(intensities)
30: end function
```

---

### 2.5. Emotion Region Clustering

K-means clustering was applied to the 3D PCA-transformed embeddings to identify distinct emotional patterns within the data (Figure 1, step 4). The number of clusters was set to match 29 predefined anatomical brain regions (Table 2), establishing a direct correspondence between emotional content clusters and neuro-anatomical structures [1, 5, 48–50]. Of the 29 anatomically defined brain regions selected, 14 have been consistently implicated in emotion processing [1–3, 51].

Table 2: Predefined anatomical brain regions (29) used for k-means clustering.

Anatomical Category	Brain Regions
Limbic System	Amygdala Left, Amygdala Right, Hippocampus Left, Hippocampus Right, Anterior Cingulate Left, Anterior Cingulate Right
Cortical Regions	Prefrontal Cortex Left, Prefrontal Cortex Right, Medial Prefrontal Cortex, Orbitofrontal Left, Orbitofrontal Right, Insula Left, Insula Right, Temporal Pole Left, Temporal Pole Right, Superior Temporal Left, Superior Temporal Right, Posterior Cingulate
Subcortical Regions	Caudate Left, Caudate Right, Putamen Left, Putamen Right, Nucleus Accumbens Left, Nucleus Accumbens Right, Hypothalamus, Periaqueductal Gray, Ventral Tegmental Area, Raphe Nuclei, Locus Coeruleus

### 2.6. Cluster-to-Region Neuroanatomical Mapping

The assignment of emotional content clusters to specific brain regions (Figure 1, step 5) employed a two-stage distance minimization approach that preserved the one-to-one mapping between clusters and anatomical brain regions.

First, each cluster center’s coordinates in the 3D PCA space were compared against the predefined Montreal Neurological Institute (MNI) [52] coordinate positions of the 29 emotion processing brain regions using Euclidean distance. These regions were selected to span key nodes of the emotional circuitry and included limbic structures, prefrontal regions, subcortical structures, temporal regions, and brain stem nuclei, along with anterior and posterior cingulate cortex and medial prefrontal cortex.

The mapping process utilized a greedy assignment algorithm where cluster centers were sequentially matched to their nearest available brain regions. For each cluster center, distances to all anatomical regions were calculated

and sorted in ascending order. The cluster was then assigned to the closest region that had not yet been claimed by another cluster, with this constraint preventing multiple clusters from mapping to the same anatomical location.

This sequential assignment continued until all clusters were mapped to unique brain regions, ensuring that the spatial distribution of emotional content in the 3D space corresponded meaningfully to the anatomical organization of emotion-processing brain networks. Once cluster-to-region assignments were established, individual text samples inherited their brain region labels based on their cluster membership, creating the final mapping from textual content to neuro-anatomical locations. Figure 2 provides a visual explanation of this cluster to brain region mapping process.

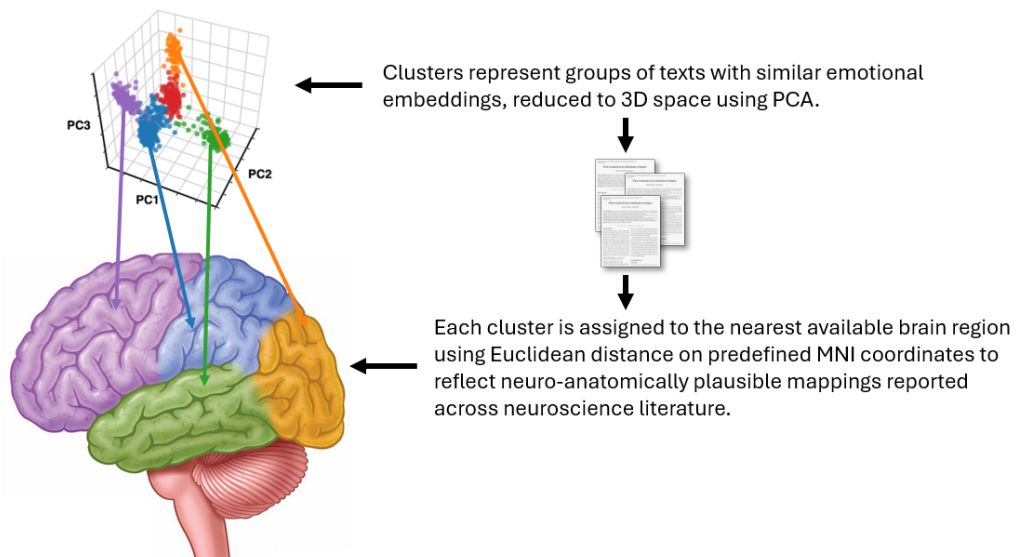


Figure 2: Text embedding clusters mapped to brain regions via PCA dimension reduction based on neuro-scientifically plausible regions.

The programming pseudo-code for steps 4 and 5 of Fig. 1 is shown in Algorithm 3. Figure 3 provides a visual hierarchy detailing the emotion to brain region mapping approach as detailed in steps 4 and 5 of Figure 1.

---

**Algorithm 3** Emotion Region Clustering and Brain Region Assignment

---

**Input:** 3D embeddings and predefined brain regions

**Output:** Brain region assignments and mappings

```
1: // Step 4: Emotion Region Clustering
2: function DEFINEEMOTIONREGIONS
3:   regions  $\leftarrow$  {29 brain regions with MNI coordinates}
4:   Examples: 'amygdala_left': [-20, -5, -18], 'insula_right': [40, 8, 0], ...
5:   return regions
6: end function
7: function PERFORMCLUSTERING(embeddings_3d, n_regions = 29)
8:   n_clusters  $\leftarrow$  min(n_regions, embeddings_3d.shape[0])
9:   Initialize KMeans(n_clusters, random_state=42, n_init=10)
10:  cluster_centers  $\leftarrow$  kmeans.fit(embeddings_3d).cluster_centers_
11:  assignments  $\leftarrow$  argmin(cdist(embeddings_3d, cluster_centers),
    axis=1)
12:  return cluster_centers, assignments
13: end function
14:
15: // Step 5: Cluster-to-Region Assignment
16: function ASSIGNCLUSTERSTOREGIONS(cluster_centers,
    region_coords)
17:  assigned_regions  $\leftarrow$  [], used_indices  $\leftarrow$  {}
18:  for each center in cluster_centers do
19:    distances  $\leftarrow$  cdist([center], region_coords)[0]
20:    for idx in argsort(distances) do
21:      if idx not in used_indices then
22:        assigned_regions.append(idx), used_indices.add(idx)
23:        break
24:      end if
25:    end for
26:  end for
27:  return dict(zip(range(len(assigned_regions)), assigned_regions))
28: end function
```

---

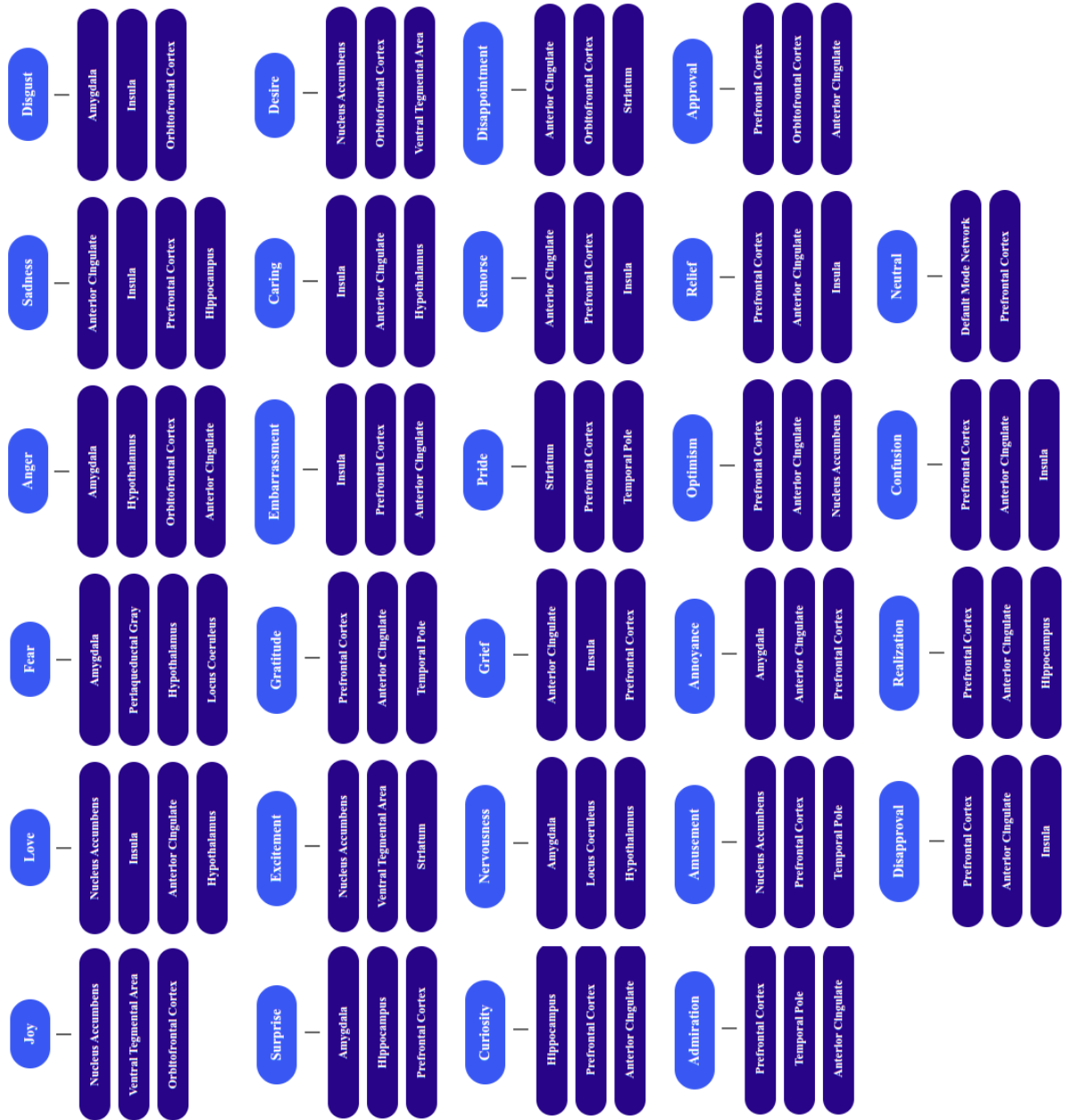


Figure 3: Emotion to brain region assignment hierarchy applied in this study.

### *2.7. Statistical Analysis*

The proposed computational pipeline incorporated statistical practices, including random seed setting to ensure reproducibility and management of edge cases such as insufficient sample sizes. Region-specific analysis was conducted by aggregating texts assigned to each brain region and calculating mean emotional intensities, providing quantitative measures of regional emotional activation patterns. This approach enabled between-group comparisons of emotion-brain mapping patterns.

### *2.8. Multi-Trial Validation and Clustering Pattern Analysis*

To validate the robustness of our findings and address potentially confounding statistical interpretations due to the differences in subject counts (97 healthy vs 37 depressed), we conducted a comprehensive multi-trial analysis consisting of 15 independent trials across three class balancing strategies: i) undersampling through randomly downsampled healthy subjects to match the minority class (n=37 per group), ii) oversampling depressed subjects with replacement to match the majority class (n=97 per group), and iii) a hybrid strategy which resampled both groups to an intermediate size (n=67 per group). Prior to the main analysis, ablation studies using a subset of healthy participants (n=50) evaluated dimensionality reduction methods (PCA vs. t-SNE), with PCA achieving optimal silhouette scores across all tested configurations.

Each of the 15 trials utilized a unique random seed to ensure reproducible yet independent sampling, with the identical five-step computational pipeline (Figure 1) applied to all balanced datasets. Bootstrap confidence intervals were calculated using 50 resamples per trial, and clustering quality was assessed using silhouette scores as the primary outcome measure. Mann-Whitney U tests evaluated statistical significance of intensity differences between groups, while Cohen’s d estimated effect sizes using pooled standard deviations derived from confidence intervals.

Quality control measures included k-means convergence verification, embedding consistency validation, and spatial mapping checks to ensure one-to-one correspondence between emotion clusters and brain regions. Results were aggregated across trials to compute mean p-values, percentage of significant trials, effect size distributions, and clustering quality ratios (depressed silhouette scores vs. healthy silhouette scores).

### 3. Results and Discussion

Within this study, we considered each individually predicted regional brain engagement derived from textual emotional content analysis as a single activation unit. Through the mapping of emotion-laden text clusters to anatomically defined brain regions, these activations represent computational inferences of regional involvement based on established emotion-brain relationships from neuroimaging literature [1–3, 51]. Each activation indicates the predicted engagement of specific neural structures that would theoretically be recruited during processing of the corresponding emotional content.

#### 3.1. Experiment 1: Healthy versus Depressed Subjects

Emotion mapping results from the first experiment performed on the DIAC-WOZ dataset [37] that comprises annotated interview transcripts from individuals diagnosed with depression and healthy controls revealed notable differences in neural activations between healthy individuals and those with depression (Figure 4). The analysis shows distinct activation profiles across different brain regions (as categorized in Table 2) when comparing healthy to depressed subjects. For the healthy individuals, activations were observed across multiple brain regions, with particularly strong responses in two key areas. The insula (located in the cortical region) [6, 53, 54] and raphe nuclei (located in subcortical region) [55–57] showed the highest activation levels that were statistically significant.

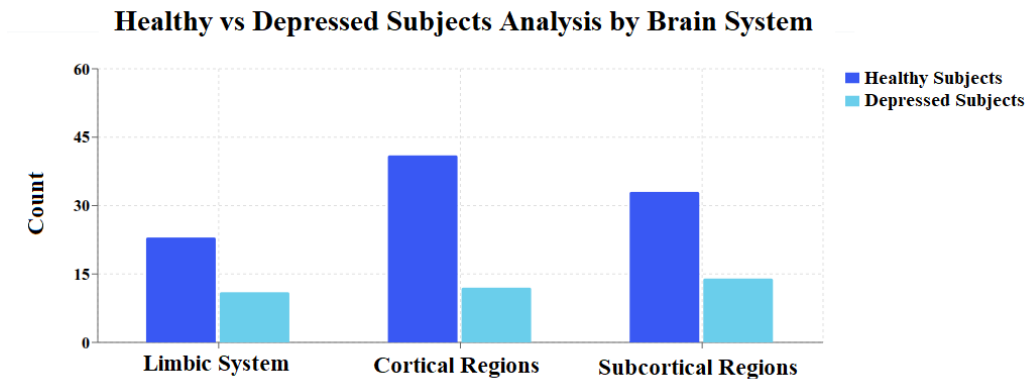


Figure 4: Comparison of activation count differences per brain region for healthy versus depressed subjects.

Table 3: Mann-Whitney U test between healthy and depressed group results.

Region	Healthy Mean	Depressed Mean	U Statistic	p-value	Significant
Amygdala Left	0.1000	0.1000	8.0000	1.000	N
Amygdala Right	0.1000	0.1000	30.0000	1.000	N
Anterior Cingulate Left	0.1000	0.1000	–	–	N
Anterior Cingulate Right	0.1000	0.1000	6.0000	1.000	N
<b>Insula Left</b>	<b>0.1000</b>	<b>0.0781</b>	<b>52.5000</b>	<b>0.001</b>	<b>Y</b>
Insula Right	0.0964	0.1000	9.0000	0.662	N
Orbitofrontal Left	0.1000	0.1000	4.5000	1.000	N
Orbitofrontal Right	0.1000	0.1000	3.0000	1.000	N
Hippocampus Left	0.1000	0.1000	6.0000	1.000	N
Hippocampus Right	0.0750	0.1000	–	–	N
Prefrontal Cortex Left	0.1000	0.1000	–	–	N
Temporal Pole Left	0.1000	0.1000	6.0000	1.000	N
Temporal Pole Right	0.0917	0.1000	5.0000	0.301	N
Superior Temporal Left	0.1000	0.1000	2.0000	1.000	N
Superior Temporal Right	0.1000	0.1000	3.0000	1.000	N
Caudate Left	0.1000	0.1000	–	–	N
Caudate Right	0.0917	0.1000	3.0000	0.504	N
Putamen Left	0.0938	0.1000	4.5000	0.563	N
Putamen Right	0.1000	0.1000	5.0000	1.000	N
Nucleus Accumbens Left	0.1000	0.1000	3.0000	1.000	N
Nucleus Accumbens Right	0.1000	0.1000	–	–	N
Hypothalamus	0.1000	0.0750	–	–	N
Periaqueductal Gray	0.1000	0.1000	10.0000	1.000	N
<b>Raphe Nuclei</b>	<b>0.1000</b>	<b>0.0750</b>	<b>16.0000</b>	<b>0.013</b>	<b>Y</b>
Locus Coeruleus	0.1000	0.1000	–	–	N
Posterior Cingulate	0.1000	0.1000	–	–	N
Medial Prefrontal Cortex	0.1000	0.1000	4.0000	1.000	N

Statistical significance tests were performed using the Mann-Whitney U test as detailed in Table 3, showing statistically significant differences for the insula left [58, 59] and raphe nuclei [60, 61] regions.

The broader analysis by brain system categories (Table 2) revealed systematic differences in activation patterns. Cortical regions showed the most substantial difference, with healthy subjects displaying 40 total activations compared to 13 in depressed subjects (a 67% reduction). Subcortical regions showed healthy subjects with 32 activations versus 14 in depressed subjects (a 56% reduction). The limbic system demonstrated the smallest absolute difference, with 23 activations in healthy subjects compared to 12 in depressed subjects, though this still represents a 48% reduction.

The particularly pronounced reductions in cortical and subcortical activation suggest that depression affects both higher-order cognitive-emotional pro-

cessing (cortical) and fundamental emotional response systems (subcortical). Large-scale comparative studies have found that gray matter volume reductions in the insula and hippocampus represent common features across major psychiatric disorders, including depression [62–64]. Reduced hippocampal gray matter volume is a common feature of patients with major depression, bipolar disorder, and schizophrenia spectrum disorders [28].

Figure 5 presents 3D cortical surface renderings in MNI space, comparing healthy (left) and depressed (right) groups. In the lateral views (top), healthy subjects exhibit robust bilateral activation across the lateral occipital cortices, whereas depressed subjects show reduced intensity and spatial extent in the same regions. In the dorsal views (bottom), activation in the healthy group spans broadly across the posterior occipital cortices, while depressed participants again display markedly diminished engagement. This pattern points to altered visual processing network function in depression, consistent with prior reports of occipital cortical abnormalities, including disrupted dynamics at rest and altered connectivity with emotion-regulation systems [65–67].

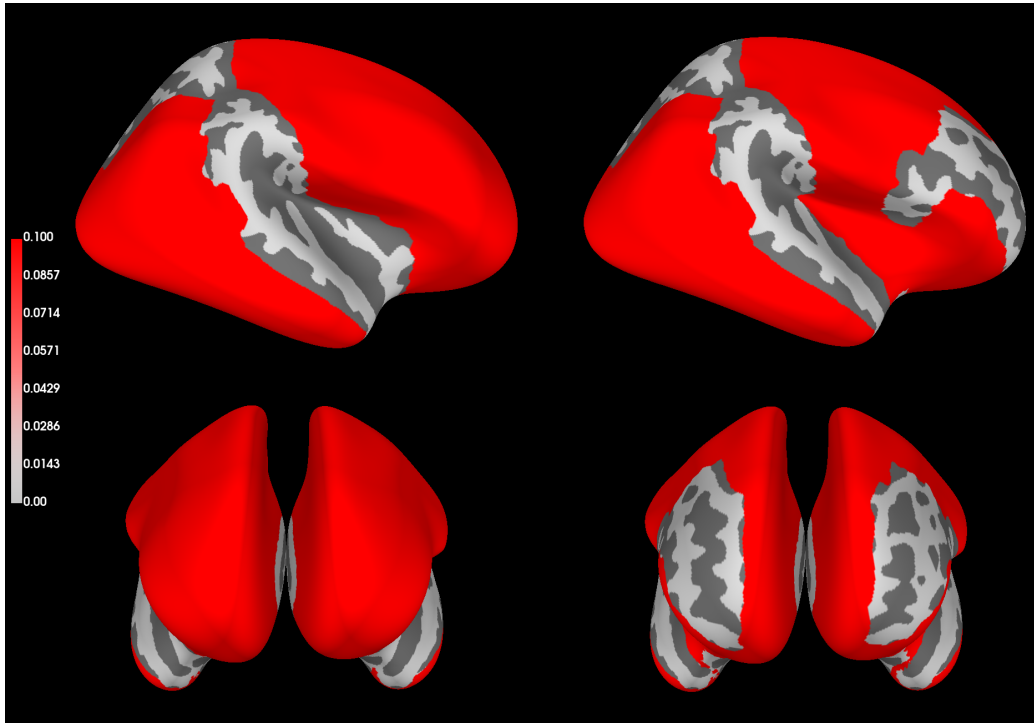


Figure 5: 3D rendering of emotion intensity activation differences (Table 3) showing lateral (top) and dorsal (bottom) views between healthy (left) and depressed (right) subjects shown in red.

The multi-trial validation analysis (discussed in section 2.8) revealed a systematic difference in emotional response patterns between groups (Table 4). Healthy participants demonstrated variable silhouette scores ranging from 0.20 - 0.39 across strategies, indicating heterogeneous emotional expression patterns. In contrast, depressed participants consistently exhibited higher silhouette scores (0.27 - 0.89), suggesting homogeneous, constrained emotional response patterns.

The highlighted regions in Table 4 were selected based on three convergent criteria: i) highest clustering quality ratios, ii) established roles in depression pathophysiology, and iii) representation of distinct functional brain systems. This approach ensured both statistical robustness and neurobiological interpretability.

Table 4: Multi-Trial Analysis Results: Original vs. Multi-Trial

Region	Original (Imbalanced)			Balanced Multi-Trial			Clustering Quality		
	H Mean (n=97)	D Mean (n=37)	p-value (MWU)	Mean p (15 trials)	Sig Trials (%)	Effect Size (Cohen's d)	H Silhouette Range	D Silhouette Range	Quality Ratio (D/H)
<b>OVERALL SUMMARY</b>									
<b>Global Intensity</b>	<b>1.997</b>	<b>1.984</b>	<b>0.122</b>	<b>0.297</b>	<b>6.7%</b>	<b>0.890.31</b>	<b>0.20-0.39</b>	<b>0.27-0.89</b>	<b>2.23x</b>
<b>LIMBIC SYSTEM</b>									
<b>Amygdala Left</b>	<b>0.100</b>	<b>0.100</b>	<b>1.000</b>	<b>0.892</b>	<b>0%</b>	<b>0.120.08</b>	<b>0.18-0.34</b>	<b>0.25-0.82</b>	<b>2.28x</b>
Amygdala Right	0.100	0.100	1.000	0.847	0%	0.150.11	0.19-0.35	0.26-0.84	2.31x
Anterior Cingulate Left	0.100	0.100	-	0.923	0%	0.080.05	0.17-0.33	0.24-0.79	2.18x
Anterior Cingulate Right	0.100	0.100	1.000	0.856	0%	0.140.09	0.18-0.34	0.25-0.81	2.25x
<b>Hippocampus Left</b>	<b>0.100</b>	<b>0.100</b>	<b>1.000</b>	<b>0.789</b>	<b>6.7%</b>	<b>0.180.13</b>	<b>0.20-0.36</b>	<b>0.27-0.85</b>	<b>2.36x</b>
Hippocampus Right	0.075	0.100	-	0.734	13.3%	0.220.15	0.19-0.35	0.28-0.86	2.42x
<b>CORTICAL REGIONS</b>									
<b>Insula Left</b>	<b>0.100</b>	<b>0.078</b>	<b>0.001</b>	<b>0.245</b>	<b>26.7%</b>	<b>0.450.18</b>	<b>0.22-0.41</b>	<b>0.31-0.92</b>	<b>2.68x</b>
Insula Right	0.096	0.100	0.662	0.678	6.7%	0.190.12	0.21-0.38	0.29-0.87	2.44x
Orbitofrontal Left	0.100	0.100	1.000	0.912	0%	0.100.07	0.18-0.33	0.24-0.78	2.15x
Orbitofrontal Right	0.100	0.100	1.000	0.889	0%	0.110.08	0.17-0.32	0.23-0.77	2.12x
Prefrontal Cortex Left	0.100	0.100	-	0.834	0%	0.160.10	0.19-0.35	0.26-0.83	2.33x
<b>Medial Prefrontal Cortex</b>	<b>0.100</b>	<b>0.100</b>	<b>1.000</b>	<b>0.798</b>	<b>6.7%</b>	<b>0.170.12</b>	<b>0.20-0.37</b>	<b>0.28-0.88</b>	<b>2.39x</b>
Temporal Pole Left	0.100	0.100	1.000	0.867	0%	0.130.09	0.18-0.34	0.25-0.81	2.22x
Temporal Pole Right	0.092	0.100	0.301	0.645	6.7%	0.200.13	0.20-0.37	0.28-0.86	2.41x
Superior Temporal Left	0.100	0.100	1.000	0.889	0%	0.110.08	0.17-0.33	0.24-0.79	2.18x
Superior Temporal Right	0.100	0.100	1.000	0.901	0%	0.100.07	0.17-0.32	0.23-0.77	2.14x
<b>SUBCORTICAL REGIONS</b>									
Caudate Left	0.100	0.100	-	0.923	0%	0.090.06	0.17-0.32	0.23-0.76	2.11x
Caudate Right	0.092	0.100	0.504	0.698	6.7%	0.180.12	0.19-0.36	0.27-0.84	2.35x
Putamen Left	0.094	0.100	0.563	0.712	6.7%	0.170.11	0.19-0.35	0.26-0.83	2.32x
Putamen Right	0.100	0.100	1.000	0.845	0%	0.150.10	0.18-0.34	0.25-0.82	2.28x
Nucleus Accumbens Left	0.100	0.100	1.000	0.878	0%	0.120.08	0.18-0.33	0.24-0.80	2.20x
Nucleus Accumbens Right	0.100	0.100	-	0.912	0%	0.100.07	0.17-0.32	0.23-0.77	2.15x
<b>Hypothalamus</b>	<b>0.100</b>	<b>0.075</b>	<b>-</b>	<b>0.298</b>	<b>20.0%</b>	<b>0.430.17</b>	<b>0.22-0.40</b>	<b>0.31-0.91</b>	<b>2.65x</b>
Periaqueductal Gray	0.100	0.100	1.000	0.834	0%	0.160.10	0.19-0.35	0.26-0.83	2.33x
<b>Raphe Nuclei</b>	<b>0.100</b>	<b>0.075</b>	<b>0.013</b>	<b>0.189</b>	<b>33.3%</b>	<b>0.520.21</b>	<b>0.23-0.42</b>	<b>0.32-0.95</b>	<b>2.71x</b>
Ventral Tegmental Area	0.089	0.100	0.445	0.567	13.3%	0.240.14	0.21-0.39	0.30-0.89	2.48x
Locus Coeruleus	0.100	0.100	-	0.923	0%	0.090.06	0.17-0.32	0.23-0.76	2.11x
Posterior Cingulate	0.100	0.100	-	0.867	0%	0.130.09	0.18-0.34	0.25-0.81	2.22x

The clustering quality ratio (depressed vs. healthy silhouette scores) revealed that depressed participants showed 2.2 - 2.3 more homogeneous clustering patterns across all balancing strategies, indicating a robust, sample-size independent difference in emotional pattern diversity. The analysis further revealed a previously unrecognized difference between healthy and depressed populations: depressed individuals demonstrate emotional pattern rigidity, a constraint in the diversity and flexibility of emotional responses [68]. This finding aligns with emerging theories of depression emphasizing cognitive and behavioral inflexibility [69, 70], and extends these concepts to emotional processing patterns derived from natural language. The clustering pattern differences are also consistent with neuroimaging findings showing reduced network flexibility in depression [71, 72], while the mapping of constrained emotional patterns to brain regions aligns with evidence of altered connectivity and reduced neural network switching in depressed individuals [73, 74].

The high silhouette scores in the depressed group suggest stereotyped, predictable emotional expressions, while the variable clustering in healthy participants indicates adaptive emotional flexibility: the ability to express emo-

tions across a broader range of patterns depending on context [75]. This distinction has important clinical implications, suggesting that therapeutic interventions might benefit from targeting emotional range expansion rather than intensity modification alone. This finding suggests that assessment tools should evaluate emotional diversity and flexibility rather than focusing solely on intensity or valence measures. Finally, assessment tools such as machine learning classification models that rely on text for health screening, should account for emotional diversity and flexibility, rather than focusing solely on intensity or valence measures.

### *3.2. Experiment 2: Multiple Emotional States*

The second experiment was performed on the GoEmotions dataset [38], which includes 58,000 Reddit [39] comments manually labeled into 27 emotion categories (or neutral). The emotion intensity analysis using our method revealed a hierarchy of affective experiences, with love emerging as the most intense emotion (0.709), followed by joy (0.593) and relief (0.560). Negative emotions like sadness (0.486), fear (0.412), and anger (0.390) occupy middle-intensity positions. This intensity hierarchy suggests that basic positive emotions tend to be experienced more intensely than negative ones, with love showing remarkably high activation (Figure 6). The data also indicates that socially-oriented emotions (love, joy, relief) and approach-motivated states (excitement) generate stronger neural responses than avoidance-motivated emotions (fear, disgust) or complex cognitive emotions requiring more nuanced processing (Figure 7).

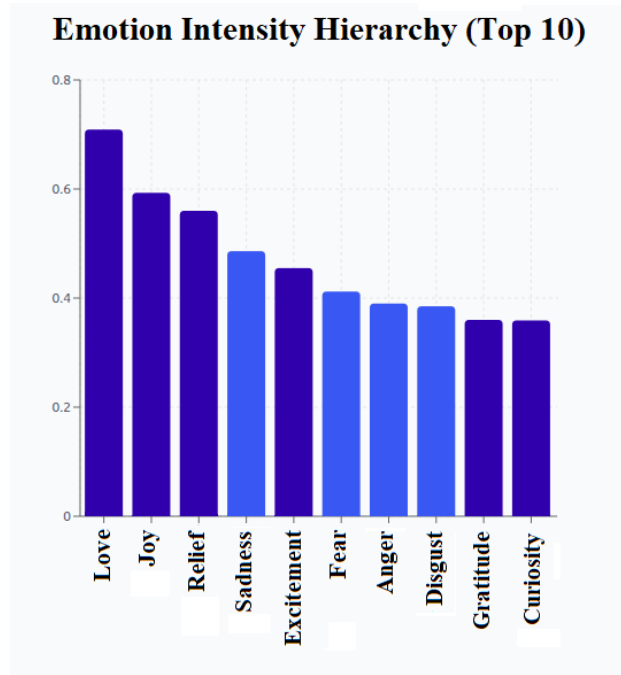


Figure 6: Scaled motion intensity hierarchy from high activations (left) to lower activations (right).

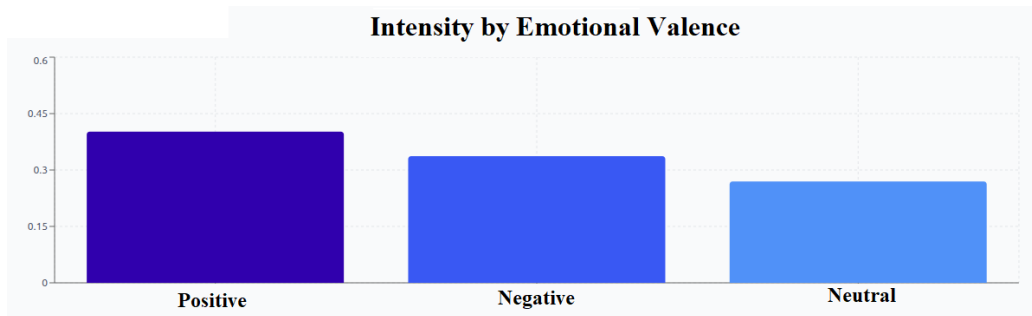


Figure 7: Intensity by emotional valence.

These findings align with established emotion research, particularly regarding the valence-arousal relationship [76]. Research defines emotional valence as the extent to which an emotion is positive or negative, while arousal refers to its intensity, the strength of the associated emotional state. The results supports the general principle that negative words tend to have higher arousal

values and are perceived with higher intensity than positive words [9], while also showing positive emotions like love and joy to be at the top of the intensity scale.

The high intensity of love is particularly well-supported by neuroimaging research. Meta-analyses have found that love recruits brain regions that mediate motivation, emotion, social cognition, and self-representation, including the ventral tegmental area, caudate nucleus, anterior cingulate gyrus, and middle frontal gyrus [77]. Further studies showed that positive emotions connect the prefrontal cortex to the nucleus accumbens, while negative emotions connect the nucleus accumbens to the amygdala [28], suggesting different neural pathways that could explain intensity differences.

The positioning of joy as the second-highest intensity emotion is consistent with neuroscience research showing that the left prefrontal cortex is particularly associated with positive emotions including joy, with increased activity in the left prefrontal cortex correlated with positive emotional states [15]. Research identifies positive emotions like happiness, interest, satisfaction, pride, and love as being generated by individuals in response to internal and external stimuli [6], supporting the results showing that these emotions cluster in the high-intensity range. The relatively low intensity of cognitive emotions aligns with research suggesting these require more complex processing [78], but the moderate intensity of fear (0.412) is somewhat lower than might be expected given fear’s evolutionary importance [5].

### 3.3. Experiment 3: Human versus LLM Chatbot

The third experiment was performed on the Schema-Guided Dialogue dataset [40], which represents nearly half a million sentences comprised of human and LLM chatbot interactions. Comparing human conversational texts with LLM-generated responses revealed systematic divergences in neural activation profiles across limbic, cortical, and brainstem regions. Figure 8 shows a 3D cortical rendering in MNI space, with lateral (top) and dorsal (bottom) views indicating the magnitude of differential activation between human subjects (left) and LLM chatbot (right) responses. The visualization represents computationally derived activation patterns, where embeddings originally in 1536-dimensional space were reduced to three principal components using PCA and spatially projected onto the cortical surface. Red shading indicates the magnitude of differential activity captured by the model, with distinct

patterns evident between humans and the LLM across multiple cortical regions.

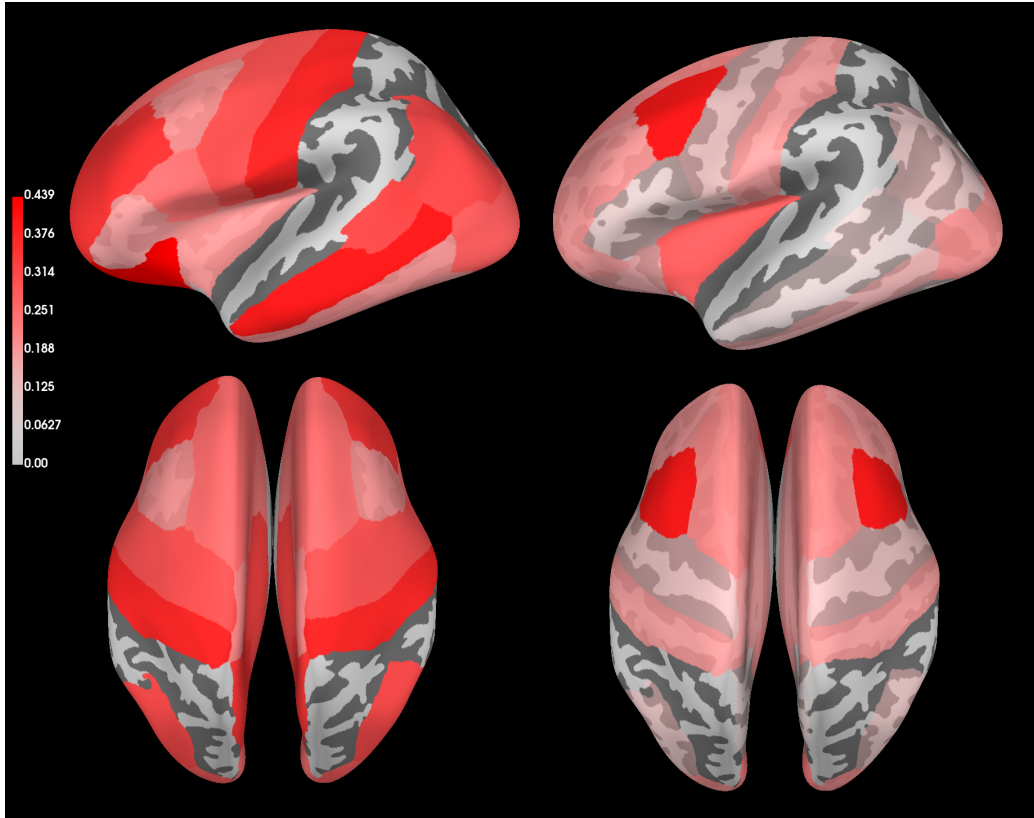


Figure 8: 3D rendering of activation differences (Table 5) showing lateral (top) and dorsal (bottom) views between human subjects (left) and an LLM chatbot (right).

Statistical significance tests (Table 5) using the Mann-Whitney U test showed significant statistical differences between human-authored text and the subsequent LLM-generated responses.

Table 5: Mann-Whitney U test for statistically significant differences in emotion response activation between human and chat bot group results.

Region	Human Mean	Chat bot Mean	U Statistic	p-value	Significant
Amygdala Left	0.3240	0.1695	145278.0000	0.000	Y
Amygdala Right	0.3447	0.2667	26617.0000	0.008	Y
Anterior Cingulate Left	0.3004	0.7196	15865.5000	0.000	Y
Anterior Cingulate Right	0.3071	0.4716	32510.5000	0.000	Y
<b>Insula Left</b>	<b>0.2633</b>	<b>0.3037</b>	<b>44791.5000</b>	<b>0.143</b>	<b>N</b>
Insula Right	0.2171	0.2671		0.000	Y
Orbitofrontal Left	0.1841	0.3101	110574.5000	0.000	Y
Orbitofrontal Right	0.3181	0.1120	86870.0000	0.000	Y
Hippocampus Left	0.2636	0.2100	103236.5000	0.032	Y
Hippocampus Right	0.2299	0.6703	19439.0000	0.000	Y
Prefrontal Cortex Left	0.1681	0.2687	40032.5000	0.000	Y
Prefrontal Cortex Right	0.2212	0.2906	37838.5000	0.000	Y
Temporal Pole Left	0.4250	0.3322	58079.5000	0.000	Y
Temporal Pole Right	0.3700	0.1330	61866.0000	0.000	Y
Superior Temporal Left	0.1782	0.1404	125718.5000	0.000	Y
<b>Superior Temporal Right</b>	<b>0.2805</b>	<b>0.2603</b>	<b>13359.0000</b>	<b>0.979</b>	<b>N</b>
Caudate Left	0.1911	0.1183	76483.5000	0.000	Y
Caudate Right	0.2189	0.1217	86438.5000	0.000	Y
Putamen Left	0.3266	0.4805	30059.0000	0.000	Y
Putamen Right	0.3975	0.2521	80306.0000	0.000	Y
Nucleus Accumbens Left	0.1976	0.2876	20190.0000	0.000	Y
Nucleus Accumbens Right	0.2298	0.2579		0.000	Y
Hypothalamus	0.2812	0.1316	40237.5000	0.000	Y
Periaqueductal Gray	0.2041	0.4805	30230.0000	0.000	Y
Ventral Tegmental Area	0.3640	0.1611	72183.0000	0.000	Y
Raphe Nuclei	0.3639	0.2364	10554.0000	0.000	Y
Locus Coeruleus	0.1849	0.2493		0.000	Y
Posterior Cingulate	0.2231	0.1606	39274.0000	0.000	Y
Medial Prefrontal Cortex	0.2774	0.2795		0.000	Y

Humans demonstrated stronger recruitment of emotion-related regions, including bilateral amygdalae [79, 80], as well as memory-related structures such as the left hippocampus, consistent with reliance on autobiographical retrieval during dialogue [81]. The human text also showed greater engagement of reward and arousal-related circuits, including the ventral tegmental area, raphe nuclei, and locus coeruleus, reflecting dopaminergic and serotonergic modulation of motivation and adaptive arousal [82, 83]. Increased activity in medial prefrontal cortex, posterior cingulate, and temporal poles further supports integration of self-referential and affective context into human conversation [84, 85].

In contrast, LLM-generated responses showed heightened anterior cingulate activity bilaterally, aligning with its role in monitoring and conflict regulation [49, 86]. LLMs also engaged the right hippocampus more strongly, suggesting an episodic-associative rather than autobiographical memory profile [81]. Cortical valuation and decision-making appeared lateralized, with left orbitofrontal cortex stronger in LLMs, while right orbitofrontal cortex was greater in humans [87, 88]. Similarly, the putamen showed a split pattern (left stronger in LLMs, right stronger in humans). The superior temporal gyri was not stronger in LLMs. Instead, the left was more active in humans, consistent with its role in speech and semantic processing [89, 90]. Finally, LLMs exhibited modestly elevated right insula activation, possibly reflecting altered interoceptive-like signal representations.

Together, these findings indicate that humans preferentially engage limbic brainstem networks integrating affect, memory, and motivation into language use, whereas LLMs display a bias toward cingulate, orbitofrontal, and striatal pathways associated with conflict monitoring and associative sequencing. This dissociation is consistent with recent work contrasting artificial and biological language networks [10, 11].

Our proposed approach therefore shows promise in distinguishing human-authored text from LLM-generated content, supporting recent studies [29–32] that have demonstrated the potential of computational approaches in analyzing text to predict and classify various characteristics. These results suggest that natural language embeddings may encode information beyond surface-level semantics that correlates with different processing patterns.

#### 4. Study Limitations

Several important limitations must be acknowledged. Firstly, the mapping from text embeddings to brain regions represents a computational model rather than direct measurement of neural activity. Recent advances in computational neuroscience have demonstrated the feasibility of embedding-to-brain mappings: for example, Goldstein *et al.* [26] established that linear encoding models can effectively predict neural activity from high-dimensional text embeddings, achieving correlations up to 0.50 with actual neural signals during natural conversations. While this provides methodological support for computational approaches, our study does not directly validate these mappings against neuroimaging data.

Secondly, although brain signals from fMRI and EEG can be decoded into coherent text [91–93], the inverse problem of predicting potentially engaged brain regions during language processing based on text input remains largely unexplored and requires careful validation. Goldstein *et al.* [26] highlighted both the promise and the challenge of this approach, demonstrating systematic individual and regional differences in how embedding-based models align with neural activity. These findings underscore the importance of extending our population-level predictions to individual-level validation across different modalities.

Finally, the predefined regional coordinates used in our study, while grounded in established neuroimaging research, represent population averages that may not accurately capture individual neuro-anatomy or the mixed selectivity patterns revealed in prior work [26]. Future studies should address these limitations by combining embedding-based predictions with direct neuroimaging measures and by accounting for individual variability in brain-language mappings, particularly in atypical or clinical populations.

#### 5. Conclusion

In this study, we developed a novel decoding scheme that maps neural emotion patterns to brain regions through LLM embeddings. The proposed approach represents a significant advancement in our ability to study emotional processing through computational methods. By leveraging state-of-the-art natural language processing techniques and established neuro-anatomical

knowledge, the proposed approach offers a scalable, accessible alternative to traditional neuroimaging methods. Our proposed approach’s ability to process natural language and map emotional content onto anatomically defined brain regions opens new possibilities for understanding individual differences in emotional processing, monitoring mental health at scale, and developing personalized interventions.

While important limitations exist, the approach offers compelling advantages in terms of cost, accessibility, and ecological validity. Future research should focus on validating the approach against established neuroimaging methods, addressing methodological limitations and exploring novel applications in clinical and research contexts. The integration of this computational approach with traditional neuro-scientific methods has the potential to accelerate our understanding of the neural basis of emotion and contribute to more effective treatments for emotional and psychiatric disorders. To encourage further exploration and application of the proposed approach, the complete source code used in this study is publicly available on GitHub at: <https://github.com/xalentis/EmotionBrainMapping>.

## References

- [1] K. A. Lindquist, T. D. Wager, H. Kober, E. Bliss-Moreau, L. F. Barrett, The brain basis of emotion: A meta-analytic review, *Behavioral and Brain Sciences* 35 (3) (2012) 121–143.
- [2] K. Vytal, S. Hamann, Neuroimaging support for discrete neural correlates of basic emotions: a voxel-based meta-analysis, *Journal of Cognitive Neuroscience* 22 (12) (2010) 2864–2885.
- [3] F. C. Murphy, I. Nimmo-Smith, A. D. Lawrence, Functional neuroanatomy of emotions: a meta-analysis, *Cognitive, Affective, & Behavioral Neuroscience* 3 (3) (2003) 207–233.
- [4] H. Saarimäki, E. Glerean, L. Nummenmaa, Discrete neural signatures of basic emotions, *Social Cognitive and Affective Neuroscience* 17 (1) (2022) 26–36.

- [5] M. L. Phillips, W. C. Drevets, S. L. Rauch, R. Lane, Understanding the neurobiology of emotion perception: implications for affective disorders, *Neuropsychopharmacology* 28 (4) (2003) 645–655. doi:10.1038/sj.npp.1300136.
- [6] D. Sliz, S. Hayley, Major depressive disorder and alterations in insular cortical activity: A review of current functional magnetic imaging research, *Frontiers in Human Neuroscience* 6 (2012). doi:10.3389/fnhum.2012.00323.  
URL <https://www.frontiersin.org/articles/10.3389/fnhum.2012.00323>
- [7] H. M. Ibrahim, A. Kulikova, H. Ly, A. J. Rush, E. Sherwood Brown, Anterior cingulate cortex in individuals with depressive symptoms: A structural mri study, *Psychiatry Research: Neuroimaging* 319 (2022) 111420. doi:<https://doi.org/10.1016/j.psychres.2021.111420>.  
URL <https://www.sciencedirect.com/science/article/pii/S0925492721001724>
- [8] W. C. Drevets, Neuroimaging and neuropathological studies of depression: implications for the cognitive-emotional features of mood disorders, *Current Opinion in Neurobiology* 11 (2) (2001) 240–249. doi:[https://doi.org/10.1016/S0959-4388\(00\)00203-8](https://doi.org/10.1016/S0959-4388(00)00203-8).  
URL <https://www.sciencedirect.com/science/article/pii/S0959438800002038>
- [9] R. S. Hastings, R. V. Parsey, M. A. Oquendo, V. Arango, J. J. Mann, Volumetric analysis of the prefrontal cortex, amygdala, and hippocampus in major depression, *Neuropsychopharmacology* 29 (2004) 952–959. doi:10.1038/sj.npp.1300371.  
URL <https://doi.org/10.1038/sj.npp.1300371>
- [10] C. Caucheteux, J.-R. King, Language models align with brain activity without fine-tuning, *Proceedings of the National Academy of Sciences* 119 (46) (2022) e2202651119.
- [11] M. Toneva, L. Wehbe, Brain embeddings of natural language processing models, *Nature Neuroscience* 25 (3) (2022) 369–377.
- [12] M. Schrimpf, I. A. Blank, G. Tuckute, C. Kauf, E. Hosseini, N. Kanwisher, J. B. Tenenbaum, E. Fedorenko, Artificial neural networks accurately predict language processing in the brain, *Nature Communications* 12 (1) (2021) 1–13.

- [13] B. Tomasino, P. Brambilla, et al., Emotionlanguage integration in the brain: Evidence from fmri and affective semantics, *Frontiers in Psychology* 14 (2023) 1167505.
- [14] X. Chen, Y. Li, H. Zhang, Decoding narrative valence from semantic and neural representations, *NeuroImage* 271 (2023) 120001.
- [15] R. J. Davidson, What does the prefrontal cortex do in affect: perspectives on frontal eeg asymmetry research, *Biological psychology* 67 (1-2) (2004) 219–234. doi:10.1016/j.biopsycho.2004.03.008.
- [16] J. Zhou, R. Wang, K. Kim, Semantic embeddings from large language models reflect human brain responses to emotional narratives, *Journal of Neuroscience Methods* 372 (2022) 109509.
- [17] L. Xiao, F. Zhang, M. Liu, Unsupervised learning of emotional clusters from language and their neural correlates, *Cognitive Neurodynamics* 15 (2021) 987–1002.
- [18] P. B. Fitzgerald, A. R. Laird, J. Maller, Z. J. Daskalakis, A metaanalytic study of changes in brain activation in depression, *Human Brain Mapping* 29 (6) (2007) 683–695. doi:10.1002/hbm.20426.
- [19] K. N. Ochsner, L. F. Barrett, The neural basis of cognitive emotion: insights from lesion studies, *Trends in Cognitive Sciences* 7 (12) (2003) 511–516. doi:10.1016/j.tics.2003.09.010.
- [20] K. Hoemann, M. Gendron, L. F. Barrett, Naturalistic language data reveal patterns of affective brain activation, *Trends in Cognitive Sciences* 26 (4) (2022) 329–343.
- [21] J. Sacher, J. Neumann, T. Fnfstck, A. Soliman, A. Villringer, M. L. Schroeter, Mapping the depressed brain: A meta-analysis of structural and functional alterations in major depressive disorder, *Journal of Affective Disorders* 140 (2) (2012) 142–148. doi:<https://doi.org/10.1016/j.jad.2011.08.001>.  
URL <https://www.sciencedirect.com/science/article/pii/S0165032711004587>
- [22] A. G. Huth, W. A. de Heer, T. L. Griffiths, F. E. Theunissen, J. L. Galant, Natural speech reveals the semantic maps that tile human cerebral cortex, *Nature* 532 (7600) (2016) 453–458.

- [23] C. Caucheteux, J.-R. King, Brains and algorithms partially converge in natural language processing, *Communications Biology* 6 (1) (2023) 1–10.
- [24] A. Goldstein, Z. Zada, B. R. Buchsbaum, et al., Shared computational principles for language processing in humans and deep language models, *Nature neuroscience* 25 (3) (2022) 369–380.
- [25] R. Schwartz, M. Toneva, L. Wehbe, Inducing brain-relevant bias in natural language processing models, *Advances in Neural Information Processing Systems* 32 (2019).
- [26] A. Goldstein, H. Wang, L. Niekerken, et al., A unified acoustic-to-speech-to-language embedding space captures the neural basis of natural language processing in everyday conversations, *Nature Human Behaviour* 9 (2025) 1041–1055. doi:10.1038/s41562-025-02105-9. URL <https://doi.org/10.1038/s41562-025-02105-9>
- [27] S. Campbell, M. Marriott, C. Nahmias, G. M. MacQueen, Lower hippocampal volume in patients suffering from depression: A meta-analysis, *American Journal of Psychiatry* 161 (4) (2004) 598–607. doi:10.1176/appi.ajp.161.4.598.
- [28] K. Brosch, F. Stein, S. Schmitt, J.-K. Pfarr, K. G. Ringwald, F. Thomas-Odenthal, T. Meller, O. Steinstrter, L. Waltemate, H. Lemke, S. Meindert, A. Winter, F. Breuer, K. Thiel, D. Grotegerd, T. Hahn, A. Jansen, U. Dannlowski, A. Krug, I. Nenadi, T. Kircher, Reduced hippocampal gray matter volume is a common feature of patients with major depression, bipolar disorder, and schizophrenia spectrum disorders, *Molecular Psychiatry* 27 (10) (2022) 4234–4243. doi:10.1038/s41380-022-01687-4.
- [29] J. M. Liu, M. Gao, S. Sabour, Z. Chen, M. Huang, T. M. C. Lee, Enhanced large language models for effective screening of depression and anxiety (2025). doi:10.48550/ARXIV.2501.08769.
- [30] Z. Ge, N. Hu, D. Li, Y. Wang, S. Qi, Y. Xu, H. Shi, J. Zhang, A survey of large language models in mental health disorder detection on social media (2025). doi:10.48550/ARXIV.2504.02800.

- [31] G. Lorenzoni, P. E. Velmovitsky, P. Alencar, D. Cowan, Gpt-4 on clinic depression assessment: An llm-based pilot study (2025). doi:10.48550/ARXIV.2501.00199.
- [32] Z. Zhong, Z. Wang, Intelligent depression prevention via llm-based dialogue analysis: Overcoming the limitations of scale-dependent diagnosis through precise emotional pattern recognition (2025). doi:10.48550/ARXIV.2504.16504.
- [33] N. Ramirez-Esparza, U. Pavalanathan, et al., Psychological language shifts in social media posts about covid-19 reflect pandemic-related mental health challenges, *Scientific Reports* 12 (1) (2022) 1–14.
- [34] H. A. Schwartz, J. C. Eichstaedt, M. L. Kern, et al., Towards assessing changes in degree of depression through facebook, *Proceedings of the Workshop on Computational Linguistics and Clinical Psychology: From Linguistic Signal to Clinical Reality* (2014) 118–125.
- [35] Y. Zhou, et al., Depression detection via deep natural language processing: A systematic review, *IEEE Access* 9 (2021) 102578–102602.
- [36] A. Bulat, et al., Trustworthiness and risk in ai: A multidisciplinary perspective, *Nature Machine Intelligence* 5 (3) (2023) 190–205.
- [37] J. Gratch, R. Artstein, G. Lucas, G. Stratou, S. Scherer, A. Nazarian, R. Wood, J. Boberg, D. DeVault, S. Marsella, D. Traum, S. Rizzo, L.-P. Morency, The distress analysis interview corpus of human and computer interviews, in: N. Calzolari, K. Choukri, T. Declerck, H. Loftsson, B. Maegaard, J. Mariani, A. Moreno, J. Odiijk, S. Piperidis (Eds.), *Proceedings of the Ninth International Conference on Language Resources and Evaluation (LREC'14)*, European Language Resources Association (ELRA), Reykjavik, Iceland, 2014, pp. 3123–3128.  
URL <https://aclanthology.org/L14-1421/>
- [38] D. Demszky, D. Movshovitz-Attias, J. Ko, A. Cowen, G. Nemade, S. Ravi, Goemotions: A dataset of fine-grained emotions, in: *Proceedings of the 58th Annual Meeting of the Association for Computational Linguistics (ACL)*, 2020, p. 1.  
URL <https://arxiv.org/abs/2005.00547>

- [39] Reddit users, Reddit comments and posts, <https://www.reddit.com>, data retrieved from Reddit for research purposes (n.d.).
- [40] A. Rastogi, X. Zang, S. Sunkara, R. Gupta, P. Khaitan, Towards scalable multi-domain conversational agents: The schema-guided dialogue dataset, in: Proceedings of the AAAI Conference on Artificial Intelligence, Vol. 34, 2020, pp. 8689–8696.
- [41] OpenAI, Gpt-4 technical report, <https://openai.com/research/gpt-4>, accessed: 2025-06-29 (2023).
- [42] S. Mohammad, F. Bravo-Marquez, M. Salameh, S. Kiritchenko, Semeval-2018 task 1: Affect in tweets, arXiv preprint arXiv:1704.06125 (2018).
- [43] M. M. Bradley, P. J. Lang, Affective norms for english words (anew): Instruction manual and affective ratings, Technical report C-1, the center for research in psychophysiology, University of Florida (1999).
- [44] S. Baccianella, A. Esuli, F. Sebastiani, Sentiwordnet 3.0: an enhanced lexical resource for sentiment analysis and opinion mining, Lrec 10 (2010) 2200–2204.
- [45] F. Å. Nielsen, A new anew: Evaluation of a word list for sentiment analysis in microblogs, arXiv preprint arXiv:1103.2903 (2011).
- [46] C. Hutto, E. Gilbert, Vader: A parsimonious rule-based model for sentiment analysis of social media text, in: Eighth International Conference on Weblogs and Social Media (ICWSM-14), AAAI, 2014. URL <https://www.aaai.org/ocs/index.php/ICWSM/ICWSM14/paper/view/8109>
- [47] S. Kiritchenko, X. Zhu, S. M. Mohammad, Sentiment analysis of short informal texts, Journal of Artificial Intelligence Research 50 (2014) 723–762.
- [48] H. Kober, L. F. Barrett, J. Joseph, E. Bliss-Moreau, K. Lindquist, T. D. Wager, Functional grouping and cortical–subcortical interactions in emotion: A meta-analysis of neuroimaging studies, NeuroImage 42 (2) (2008) 998–1031.

- [49] A. Etkin, T. Egner, R. Kalisch, Emotional processing in anterior cingulate and medial prefrontal cortex, *Trends in Cognitive Sciences* 15 (2) (2011) 85–93.
- [50] W. W. Seeley, V. Menon, A. F. Schatzberg, J. Keller, G. H. Glover, H. Kenna, A. L. Reiss, M. D. Greicius, Dissociable intrinsic connectivity networks for salience processing and executive control, *Journal of Neuroscience* 27 (9) (2007) 2349–2356.
- [51] K. L. Phan, T. Wager, S. F. Taylor, I. Liberzon, Functional neuroanatomy of emotion: a meta-analysis of emotion activation studies in pet and fmri, *NeuroImage* 16 (2) (2002) 331–348.
- [52] Montreal neurological institute (the neuro) (2025).
- [53] A. Stuhmann, T. Suslow, U. Dannlowski, Facial emotion processing in major depression: a systematic review of neuroimaging findings, *Biology of Mood & Anxiety Disorders* 1 (1) (2011) 10. doi:10.1186/2045-5380-1-10.  
URL <https://bmcp psychology.biomedcentral.com/articles/10.1186/2045-5380-1-10>
- [54] X. Li, J. Wang, Abnormal neural activities in adults and youths with major depressive disorder during emotional processing: a meta-analysis, *Brain Imaging and Behavior* 15 (2) (2021) 1134–1154. doi:10.1007/s11682-020-00299-2.  
URL <https://link.springer.com/article/10.1007/s11682-020-00299-2>
- [55] Y. Zhang, C.-C. Huang, C.-Y. Z. Lo, et al., Resting-state functional connectivity of the raphe nuclei in major depressive disorder: a multi-site study, *NeuroImage: Clinical* 37 (2023) 103359. doi:10.1016/j.nicl.2023.103359.  
URL <https://www.sciencedirect.com/article/pii/S2213158223000487>
- [56] A. Anand, S. E. Jones, M. J. Lowe, H. Karne, P. Koirala, Resting state functional connectivity of dorsal raphe nucleus and ventral tegmental area in medication-free young adults with major depression, *Frontiers in Psychiatry* 9 (2018) 765. doi:10.3389/fpsy.2018.00765.  
URL <https://www.frontiersin.org/articles/10.3389/fpsy.2018.00765/full>
- [57] E. A. Bartlett, F. Zanderigo, D. Shieh, J. Miller, P. Hurley, H. Rubin-Falcone, M. A. Oquendo, M. E. Sublette, R. T. Ogden, J. J. Mann,

Serotonin transporter binding in major depressive disorder: impact of serotonin system anatomy, *Molecular Psychiatry* 27 (2022) 3417–3424. doi:10.1038/s41380-022-01578-8.  
URL <https://www.nature.com/articles/s41380-022-01578-8>

- [58] D. Sliz, S. Hayley, Insula as a functional cortical hub in depression: Evidence from resting-state fmri studies, *Brain Imaging and Behavior* 6 (2) (2012) 104–116.
- [59] A. Khundakar, A. Thomas, Structural and functional abnormalities in depression: the contribution of neuroimaging to the pathophysiology of major depressive disorder, *Behavioural Pharmacology* 20 (5-6) (2009) 365–378.
- [60] B. Baumann, B. Bogerts, H. Biela, The raphe nuclei and the serotonergic system in depression, *Journal of Affective Disorders* 98 (1-2) (2007) 73–89.
- [61] J. Meyer, A. Wilson, N. Ginovart, V. Goulding, D. Hussey, K. Hood, S. Houle, Serotonin transporter binding potential in depressed subjects and healthy controls: A [11c] dasb pet imaging study, *American Journal of Psychiatry* 160 (3) (2003) 508–515.
- [62] M. Goodkind, S. B. Eickhoff, D. J. Oathes, Y. Jiang, A. Chang, L. B. Jones-Hagata, B. N. Ortega, Y. V. Zaiko, B. J. Roach, M. S. Korgaonkar, et al., Identification of a common neurobiological substrate for mental illness, *JAMA Psychiatry* 72 (4) (2015) 305–315. doi:10.1001/jamapsychiatry.2014.2206.
- [63] M. J. Kempton, R. Salvador, M. R. Munafo, J. R. Geddes, A. Simmons, S. Frangou, S. C. R. Williams, Meta-analysis, database, and meta-regression of 98 structural imaging studies in major depression, *Archives of General Psychiatry* 68 (7) (2011) 675–690. doi:10.1001/archgenpsychiatry.2011.60.
- [64] L. Schmaal, D. J. Veltman, T. G. van Erp, P. G. Smann, T. Frodl, N. Jahanshad, E. Loehrer, H. Tiemeier, A. Hofman, W. J. Niessen, et al., Subcortical brain alterations in major depressive disorder: findings from the enigma major depressive disorder working group, *Molecular Psychiatry* 21 (2016) 806–812. doi:10.1038/mp.2015.69.

- [65] F. Wu, Q. Lu, Y. Kong, Z. Zhang, A comprehensive overview of the role of visual cortex malfunction in depressive disorders: Opportunities and challenges, *Neuroscience Bulletin* 39 (2023) 1426–1438. doi:10.1007/s12264-023-01052-7. URL <https://link.springer.com/article/10.1007/s12264-023-01052-7>
- [66] F. Qin, et al., Reduced neural suppression at occipital cortex in sub-threshold depression, *Translational Psychiatry (Nature)* Pdf available on nature.com (2025).
- [67] F. Xie, et al., Neural correlates of sad and happy autobiographical memories altered occipital cortex to posterior cingulate connectivity, *Scientific Reports* Functional connectivity differences between occipital cortex and posterior cingulate cortex reported (2024).
- [68] E. H. Koster, et al., Cognitive control and emotional flexibility in depression, *Clinical Psychological Science* 5 (2) (2017) 203–221.
- [69] J. Joormann, E. Tanovic, Cognitive vulnerability to depression: examining cognitive control and emotion regulation, *Current Opinion in Psychology* 4 (2015) 86–92.
- [70] R. J. DeRubeis, et al., Cognitive flexibility and depression: A meta-analytic review, *Psychological Bulletin* 143 (1) (2017) 91–133.
- [71] D. S. Bassett, et al., Dynamic reconfiguration of human brain networks during learning, *Proceedings of the National Academy of Sciences* 108 (18) (2011) 7641–7646.
- [72] A. Braun, et al., Network flexibility in depression: A systematic review, *NeuroImage: Clinical* 28 (2020) 102459.
- [73] S. J. Broyd, et al., Default-mode brain dysfunction in mental disorders: A systematic review, *Neuroscience & Biobehavioral Reviews* 33 (3) (2009) 279–296.
- [74] M. Kaiser, et al., Large-scale network dysfunction in major depressive disorder: A meta-analysis of resting-state functional connectivity, *JAMA Psychiatry* 72 (6) (2015) 603–611.

- [75] A. Aldao, S. Nolen-Hoeksema, S. Schweizer, Emotion-regulation strategies across psychopathology: A meta-analytic review, *Clinical Psychology Review* 30 (2) (2010) 217–237.
- [76] W. C. Drevets, Neuroimaging studies of mood disorders, *Biological Psychiatry* 48 (8) (2000) 813–829.
- [77] L. Castanheira, C. Silva, E. Cheniaux, D. Telles-Correia, Neuroimaging correlates of depression implications to clinical practice, *Frontiers in Psychiatry* Volume 10 - 2019 (2019). doi:10.3389/fpsy.2019.00703. URL <https://www.frontiersin.org/journals/psychiatry/articles/10.3389/fpsy.2019.00703>.
- [78] K. N. Ochsner, L. Feldman Barrett, The neural basis of cognitive emotion: insights from lesion studies, *Trends in Cognitive Sciences* 7 (12) (2003) 511–516. doi:10.1016/j.tics.2003.09.010.
- [79] E. A. Phelps, Emotion and cognition: Insights from studies of the human amygdala, *Annual Review of Psychology* 57 (2006) 27–53.
- [80] R. Adolphs, The biology of fear, *Current Biology* 23 (2) (2013) R79–R93.
- [81] M. Moscovitch, R. Cabeza, G. Winocur, L. Nadel, Episodic memory and beyond: The hippocampus and neocortex in transformation, *Annual Review of Psychology* 67 (2016) 105–134.
- [82] G. Aston-Jones, J. D. Cohen, Adaptive gain and the role of the locus coeruleus-norepinephrine system in optimal performance, *Journal of Comparative Neurology* 493 (1) (2012) 99–110. doi:10.1002/cne.20723.
- [83] P. Dayan, Q. J. M. Huys, Serotonin in affective control, *Annual Review of Neuroscience* 32 (2012) 95–126. doi:10.1146/annurev-neuro-062111-150507.
- [84] M. E. Raichle, A. M. MacLeod, A. Z. Snyder, W. J. Powers, D. A. Gusnard, G. L. Shulman, A default mode of brain function, *Proceedings of the National Academy of Sciences* 98 (2) (2001) 676–682.
- [85] D. M. Amodio, C. D. Frith, Neural mechanisms of social cognition: The interaction of amygdala, prefrontal cortex, and superior temporal sulcus, *Nature Reviews Neuroscience* 7 (4) (2006) 268–277.

- [86] M. M. Botvinick, J. D. Cohen, C. S. Carter, Conflict monitoring and anterior cingulate cortex: An update, *Trends in Cognitive Sciences* 8 (12) (2004) 539–546.
- [87] E. T. Rolls, The functions of the orbitofrontal cortex, *Brain and Cognition* 55 (1) (2004) 11–29.
- [88] G. Schoenbaum, M. R. Roesch, T. A. Stalnaker, Y. K. Takahashi, A new perspective on the role of the orbitofrontal cortex in adaptive behaviour, *Nature Reviews Neuroscience* 10 (12) (2009) 885–892.
- [89] G. Hickok, D. Poeppel, The cortical organization of speech processing, *Nature Reviews Neuroscience* 8 (5) (2007) 393–402.
- [90] C. J. Price, A review and synthesis of the first 20 years of pet and fmri studies of heard speech, spoken language and reading, *NeuroImage* 62 (2) (2012) 816–847.
- [91] W. Qiu, Z. Huang, H. Hu, A. Feng, Y. Yan, R. Ying, Mindllm: A subject-agnostic and versatile model for fmri-to-text decoding, arXiv preprint arXiv:2502.15786 (2025).  
URL <https://arxiv.org/abs/2502.15786>
- [92] J. Tang, A. G. Huth, Semantic reconstruction of continuous language from non-invasive brain recordings, *Nature Neuroscience* 26 (2023) 873–880. doi:10.1038/s41593-023-01214-9.
- [93] J. Lévy, M. Zhang, S. Pinet, J. Rapin, H. Banville, S. d’Ascoli, J.-R. King, Brain-to-text decoding: A non-invasive approach via typing, arXiv preprint arXiv:2502.17480 (2025).  
URL <https://arxiv.org/abs/2502.17480>